ICA News letter, 2003-2004

Charge Density Analysis on Molecular Crystals via Accurate X-ray Diffraction Data

P. Munshi and T. N. Guru Row

Solid State and Structural Chemistry Unit

Indian Institute of Science

Bangalore 560012

Introduction:

Recent advances in technology and high-speed computation has put single crystal X-ray diffraction technique on a firm pedestal as a provider of unequivocal information on both molecular and crystal structure. Continued technical developments are being made to make X-ray diffraction a unique tool for the determination of charge density distribution in molecular crystal. On one hand, methods to solve and refine very large structures have been developed to make inroads into biological realm while on the other experimental probes to unravel the features of charge densities in the intra and intermolecular regions in crystal structures. Macromolecular crystallography has reached now a stage of perfection with more and more large structures being added while the latter area is still under development. It is expected that charge density analysis will provide a firm basis for the evaluation of intermolecular features, which involve energies of the order of a few kilocalories and less.

Experimental and theoretical charge densities can be used to analyze a range of problems of chemical[1] and physical[2] interest since the charge density is a physically observable quantity. Recent technological developments in area detectors provide faster means of obtaining such quality data sets in quick time[3, 4, 5] rather than a week or a month. Data sets using conventional generators equipped with high sensitivity 2D CCD (2-dimensional Charge- Coupled Device) detectors and Oxford cryo-system to generate temperatures around 100K are becoming popular for the accumulation of redundant high quality data from molecular crystals[6, 7, 8]. One of the most exciting applications of charge

density analysis is the evaluation of one-electron properties in molecular crystals. There are a number of books[1, 2] and review articles[9, 10] which describe the different experimental and theoretical approach of charge density analysis and hence the study of different properties. The widely used approach for this purpose is the Hansen–Coppens formalism[11] in which the individual atomic densities are described in terms of a spherical core and valence densities together with an expansion of atom centered spherical harmonic functions. Also, the topology of the charge density manifests as local maxima at the positions of the nuclei as can be inferred from Bader's quantum theory of *Atoms in Molecules*[12]. The maxima of the electron density are then the *critical points* at which the first derivatives of the density become zero. The second derivative of the density, the *Laplacian* will represent the chemical features of the molecule.

Experimental Aspects:

Data collection for charge density analysis is not a routine feature. It has to be done on a good quality crystal, which diffracts well beyond the limiting sphere. For example diffraction data up to $\sin\theta/\lambda \approx 1.00$ Å^{-1} must be collected in case of MoK_α radiation. Irrespective of the crystal system it is always better to collect the full sphere data set and the merging R-factors should be as good as 1.5-3 %. This would hence become a serious rate-limiting step in case of organic molecular crystals. The following gives the methodology followed in case of charge density analysis of 2-thiocoumarin[13].

A good quality crystal (0.60 × 0.37 × 0.10 mm.) was selected for the X-ray diffraction study and was mounted in a Lindemann capillary of diameter 0.5 mm. An initial data collection on the Bruker AXS SMART APEX CCD based diffractometer (50 kV, 35 mA) at room temperature with MoK_α radiation confirmed the space group to be $P2_12_12_1$ (No. 19). The detector was positioned at 6.03 cm from the crystal. As the room temperature crystal structure was good quality and was diffracting very intensely at higher angles, the same sample was cooled to 90K (ramp rate 120K/hr) with an Oxford Cryostream N_2 open-flow cryostat. The crystal was allowed to stabilize at 90K for an hour and the unit-cell parameters were determined every 15 minutes there after until the estimated standard deviations in cell dimensions did not vary beyond acceptable limits. Three batches of data were collected as follows: the first one covered the whole sphere of

reciprocal space up to ~55^0 in 2θ covering the low θ range, the second higher order batch was up to ~77^0 in 2θ and the final high order was up to ~100^0 in 2θ. For each set, a total of 2424 frames were collected with a scan width of 0.3^0 in ω and an exposure time of 15s, 30s and 45s per frame respectively. The details of the data-collection strategy are summarized in Table 1.

Table 1. A summary of the 90K X-ray data collection strategy

Sets	Run#	$2\theta(^0)$	$\omega(^0)$	$\phi(^0)$	$\chi(^0)$	Axis	Width(^{0})	#Frames	Time(Sec.)*
SET I	01	-25	-25	0	54.79	2	0.3	606	15
	02	-25	-25	90	54.79	2	0.3	606	15
	03	-25	-25	180	54.79	2	0.3	606	15
	04	-25	-25	270	54.79	2	0.3	606	15
SET II	05	-50	-50	0	54.79	2	0.3	606	30
	06	-50	-50	90	54.79	2	0.3	606	30
	07	-50	-50	180	54.79	2	0.3	606	30
	08	-50	-50	270	54.79	2	0.3	606	30
SET III	09	-75	-75	0	54.79	2	0.3	606	45
	10	-75	-75	90	54.79	2	0.3	606	45
	11	-75	-75	180	54.79	2	0.3	606	45
	12	-75	-75	270	54.79	2	0.3	606	45

*Depending on the diffraction intensities the exposure time can be varied.

The entire data set consisting of 7272 frames were collected over a period of ~80 hrs and monitored with *SMART* software package[14]. The frames were then integrated with the *SAINT*[14] using a narrow frame integration method. A total of 9651 reflections were used for the determination of the unit cell parameters. Of the 37982 reflections from the *SAINT* output, 37879 were accepted for sorting, averaging and scaling by the program *SORTAV*[15]. Of the 37879 integrated reflections, 2053 were rejected as outliers and 35826

reflections were accepted. 642 reflections were measured only once, 1543 were measured twice and 5423 were measured three or more times. After merging a total of 7608 unique reflections to a resolution of $\sin\theta/\lambda$ = 1.08 Å^{-1} (D_{min} = 0.46 Å) were recovered to an overall completeness of 99.2%. All 35826 intensities were corrected for decay, beam inhomogeneity and absorption effects (T_{min} = 0.808, T_{max} = 0.964). The internal agreement factor for the final data set, is R_{int} = 0.038 and R_{sigma}= 0.0207. No problem from the $\lambda/2$ contamination appeared in the entire data set.

Refinement details:

Fig. 1 gives the *ORTEP*[16] diagram together with the numbering of the atoms. The refinements via *SHELXL*[17] were based on F^2 and performed using all 7608 reflections, which converged at $R(F)$ = 0.033, $wR(F)$ = 0.088 and g.o.f. = 1.036. Fig. 2 shows the packing of the molecules in the crystal lattice.

The aspherical atom refinement was based on F and carried out using the *XD* package[18], on 6908 reflection with $I > 3\sigma(I)$. The multipole refinement, which is a least squares refinement technique, based on the Hansen-Coppens multipole formalism[11] forms the basis of the *XD* package. The higher order refinement was performed using 3838 reflection with 0.8 < $\sin\theta/\lambda$ < 1.08 Å^{-1} and $I > 3\sigma(I)$, resulting in accurate positional coordinates and thermal parameters for all non H-atoms. Further, multipolar refinement was carried out using all 6908 reflections with $I > 3\sigma(I)$ in the following manner. Initially scale factor and monopole populations for all atoms were refined followed by a single κ refinement. However, the positions of the H-atoms in this refinement as well as in the subsequent refinements were fixed using the reset bond option, which constraints the hydrogen atoms to average bond distance values determined from neutron diffraction studies[19]. Refinements releasing dipole, quadrupole, octapole and hexadecapole (hexadecapole for only sulfur and oxygen atoms) populations with single κ were performed in a stepwise manner. At each step the refinements were cycled till convergence. Finally a single κ' was refined for each species for all non H-atoms along with the rest of the parameters. During the refinements no extinction correction was applied. Tests on isotropic *type1* and *type2* corrections did not significantly change the quality of the residual maps.

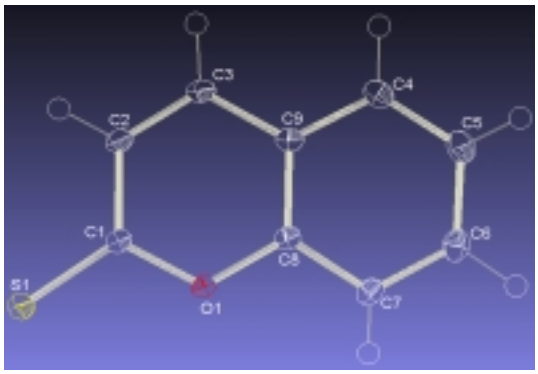

Figure 1. *ORTEP* diagram of the molecule at50% probability

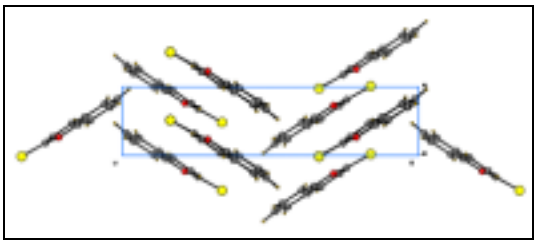

Figure 2. Molecular packing of the crystal, viewed down the *b*-axis

Discussion:

At the final convergence limit the reliability indices are as follows: $R(F) = 0.022$, $wR(F) = 0.022$ and g.o.f. = 1.81 for 6908 observed reflections. The DMSDA values[20] at this stage are good suggesting the quality of the refinement and that of the data set are excellent (maximum $\triangle Z^2 = 5 \times 10^{-4}$ Å^2 for C8-C7 bond). Also, the residual density map (Fig. 3) in the plane of the molecule obtained in the final cycle of refinement indicates the good quality of the final model. The minimum and maximum values for the residual density obtained *via XDFOUR* were -0.276 and 0.199 eÅ^{-3} respectively with the root-mean-square value of the map was 0.058 eÅ^{-3}. The code XDFFT can be used to search the maximum and minimum values of residual density in the unit cell. The experimental dynamic deformation density map given in Fig. 4 is calculated using 3955 reflections per octant. The corresponding static deformation density map, calculated based on the difference between the atom-centered multipole density and the charge distribution of the pro-molecule density, is given in Fig. 5. The later can be obtained *via XDPROP* and *XDGRAPH*. Fig. 6 shows the theoretical deformation density map, which can be generated *via GAUSSIAN98*[21] and *MOLDEN*[22] and compared with the static deformation density map. The lone pairs on the sulfur and the oxygen atoms are clearly visible in these deformation maps. The topological properties via *XDPROP* and *TOPXD* and hence

the values of bond critical point, Laplacian, bond ellipticity, bond order and bond path are reported elsewhere[13]. Fig. 7 shows the Laplacian map. The corresponding theoretical values (not given here) using HF and DFT methods with different level and map (Fig. 8) were obtained *via GAUSSIAN98* and *MORPHY*[23].

Conclusion:

The description of the methodology with the example of 2-thiocoumarin gives the general approach for charge density analysis in molecular crystals.

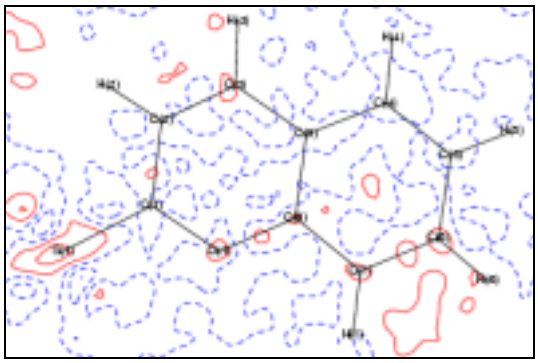

Figure 3. Residual density map, contour starts at 0.05 eÅ^{-3}, the contour levels at 0.1 eÅ^{-3} intervals. Positive contours with solid red line and negative contours with broken blue line.

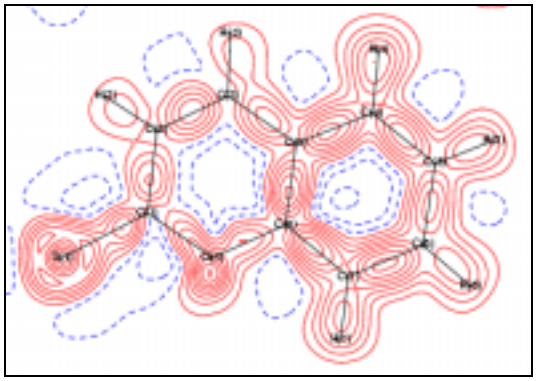

Figure 4. Dynamic deformation density map, contours are same as residual density map.

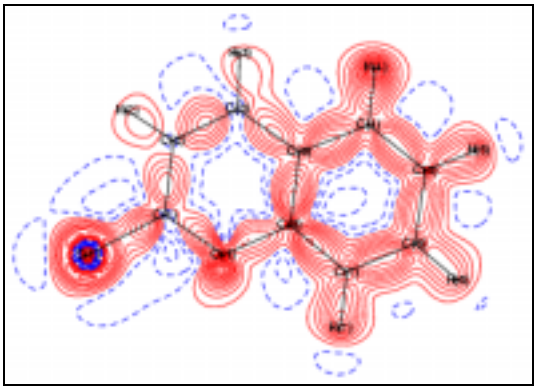

Figure 5. Static deformation density map, contours are at 0.1 eÅ^{-3} intervals. Contour colors are same as previous one.

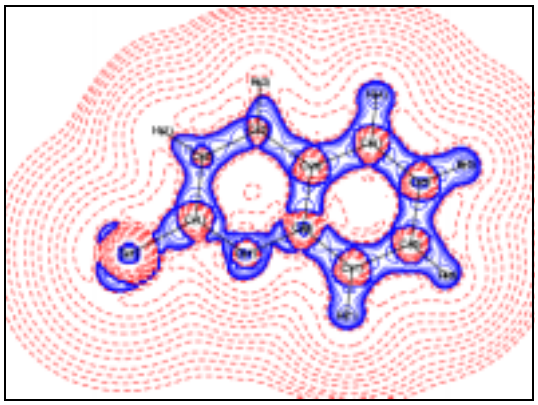

Figure 6. Theoretical deformation density map, the contours are at 0.1 eÅ^{-3} intervals. Positive contours with blue line and negative contours with red.

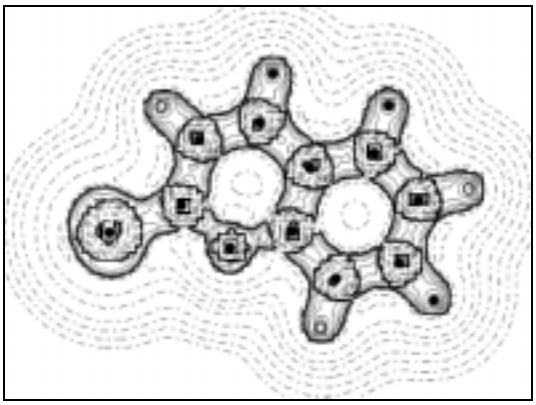

Figure 7. Laplacian [$\nabla^2\rho(\mathbf{r})$] distribution in the plane of the molecule, contours are drawn at logarithmic intervals in [$-\nabla^2\rho(\mathbf{r})$] eÅ^{-5}. Positive contours with solid blue line and negative contours with broken red.

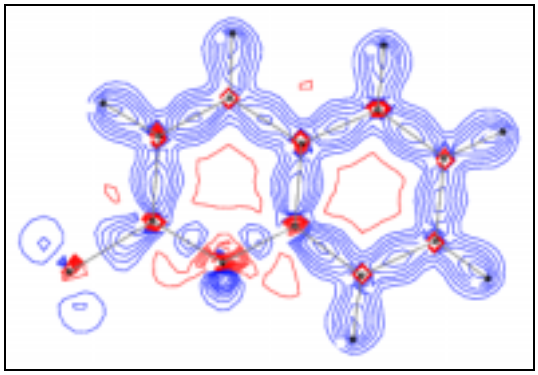

Figure 8. Theoretical Laplacian map, countours are same as experimental. Positive contours with solid line and negative contours with broken line.

References:

1. Coppens, P. (1997). *X-ray Charge Densities and Chemical Bonding*, New York: Oxford University Press.

2. Tsirel'son, V. G.; Ozerov, R. P. (1996). *Electron Density and Bonding in crystals*; Institue of Physics Publishing: Bristol.

3. Martin, A. & Pinkerton, A. A. (1998). *Acta Cryst*. B54, 477.

4. Dahaoui, S., Jelsch, C., Howard, J. A. K. & Lecomte, C. (1999). *Acta Cryst*. B55, 226.

5. Volkov, A., Wu, G. & Coppens, P. (1999). *J. Synchrotron Rad*. 6, 1007.

6. Coppens, P., Abramov, Y., Carducci, M., Korjov, B., Novozhilova, I., Alhmbra, C. & Pressprich, M. R. (1999). *J. Am. Chem. Soc.* 121, 2585.

7. Ellena, J., Goeta, A. E., Howard, J. A. K. & Punte, G. (2001). *J. Phys. Chem. A.* 105, 8696.

8. Slouf, M., Holy, A., Petricek, V. & Csarova, I. (2002). *Acta Cryst*. B58, 519.

9. (a) Spackman, M. A. (1992). *Chem Rev.* 92, 1769. (b) Spackman, M. A. and Brown, A. S. (1994). *Annu. Rep. Prog. Chem., Sect. C.: Phys. Chem.* 91, 175. (c) Spackman, M. A (1997). *Annu. Rep. Prog. Chem., Sect. C.: Phys. Chem.* 94, 177.

10. Coppens, P. and Koritsanszky, T. (2001), *Chem Rev.* 101, 1583.

11. Hansen, N. K. & Coppens, P. (1978). *Acta Cryst*. A34, 909.

12. Bader, R. F. W. (1990). *Atoms in Molecules- A Quantum Theory*, Clarendon, Oxford.

13. (a) Munshi, P. & Guru Row, T. N. (2002). *Acta Cryst*. B58, 1011. (b) Munshi, P. & Guru Row, T. N. (2003), *Acta Cryst*. B59, 159.

14. Bruker (1998). *SMART* and *SAINT*. Bruker AXS Inc., Madison, Wisconsin, USA.

15. Blessing, R. H. (1987). *Crystallogr. Rev.* 1, 3.

16. Farrugia, L. J. (1997). *J. Appl. Cryst*. 30, 565.

17. Sheldrick, G. M. (1997). *SHELXL97*. University of Göttingen, Germany.

18. Koritsanszky, T., Howard, S., Su, Z., Mallinson, P. R., Richter, T. & Hansen, N. K. (1999). *XD- Computer Program Package for Multipole Refinement and Analysis of Electron Densities from Diffraction Data*; Free University of Berlin: Berlin, Germany.

19. Allen, F. H. (1986). *Acta Cryst*. B42, 515.

20. Hirshfeld, F. L. (1976). Acta Cryst. A32, 239-244.

21. Frisch e*t. al.*(2002) *GAUSSIAN98* Revision A.11.3, Gaussian, Inc., Pittsburgh, PA.

22. Schaftenaar, G. and Noordik, J. H. (2000) *MOLDEN* (version 3.7) *J. Comput.-Aided Mol. Des.* **14**, 123-134.

23. Popelier, P. L. A. (1998). *MORPHY98*, a program written by P. L. A. Popelier with a contribution from R. G. A. bone, UMIST, Manchester, England, EU.